PHYSICAL REVIEW B VOLUME 58, NUMBER 20 15 NOVEMBER 1998-II

Theory of Auger neutralization and deexcitation of slow ions at metal surfaces

M. A. Cazalilla
Materialen Fisika Saila, Kimika Fakultatea, 1072 Postakutxatila, Euskal Herriko Unibertsitatea, 20080 Donostia, Spain

N. Lorente
Laboratoire des Collisions Atomiques et Moléculaires, Unité associée au CNRS, URA 0281, Bâtiment 351, Université de Paris-Sud, 91405 Orsay CEDEX, France

R. Díez Muiño
Laboratoire de Physico-Chimie Moléculaire, UMR 5803 CNRS, Université de Bordeaux I, Cours de la Libération, 33405 Talence CEDEX, France

J.-P. Gauyacq and D. Teillet-Billy
Laboratoire des Collisions Atomiques et Moléculaires, Unité associée au CNRS, URA 0281, Bâtiment 351, Université de Paris-Sud, 91405 Orsay CEDEX, France

P. M. Echenique
Materialen Fisika Saila, Kimika Fakultatea, 1072 Postakutxatila, Euskal Herriko Unibertsitatea, 20080 Donostia, Spain and Unidad Asociada al Instituto de Ciencia de Ciencia de Materiales, C.S.I.C., Cantoblanco, 28049 Madrid, Spain

(Received 3 June 1998)

The contribution of conduction electrons to the Auger neutralization rate of a slow ion at a metal surface has been calculated. We have considered the scattering of He^+ on Al and studied the effect of the ion potential on the neutralization rate. This has been accomplished by taking into account the modification of the wave function of the captured electron induced by the presence of the ion. The effect of the ion potential is shown to increase the Auger neutralization rate. We have also calculated the Auger deexcitation of He* $(n=2)$ atoms in front of an aluminum surface, including the distorsion created by the surface on the atom states. In this case, the deexcitation rate is reduced by the mixing of atom and surface states, which also leads to a nonvanishing deexcitation rate of metastable He (2^1S). [S0163-1829(98)06543-6]

I. INTRODUCTION

Auger neutralization of slow ions was developed as a tool to investigate the electronic structure of solid surfaces:[1] A beam of ions of low kinetic energy is scattered off a solid surface, and depending on the values of the surface work function and the ionization potentials of the projectile, electrons can be emitted when the neutralization of part of the incoming ions takes place. By analyzing the spectrum of emitted electrons, one expects to obtain information about the electronic density of states at the surface of the target. However, when a slow ion approaches a surface, it attracts the metal electrons leading to a local modification of the surface-potential barrier. Even for a singly charged ion as He^+, the perturbation is not negligible. It turns out that the energy spectrum of emitted electrons depends, not only on the local density of states, but also on the collision dynamics. It is therefore necessary to study how the interpretation of the experiments is affected by the perturbation that the ion introduces at the surface. A good starting point for such an investigation is to look at the neutralization rate of the ions. Although not directly measurable, this is one of the basic parameters required to fit the experimental data. We report here on the results of a calculation of the neutralization rate of a slow He^+ ion impinging on an aluminum surface. In this paper, the perturbation of the surface by the ion has been taken into account in a more consistent way than in previous treatments.

Investigation of charge-transfer phenomena between ions and surfaces is relevant not only to surface spectroscopy, but to many other fields. For instance, in achieving the conditions for nuclear fusion by magnetic confinement, one of the factors that govern the density of the plasma is the dynamics of charge exchange between the plasma and the reactor (tokamak) walls.[2] Indeed, only the ions neutralized by colliding with the walls can get back into the plasma. Moreover, the energy lost by an ion moving through a solid depends on the evolution of the ion charge state along its trajectory.[3] In surface chemistry, charge tranfer is involved in many surface processes and its study can help to evaluate the reactivity and other chemical properties of a given surface.

In an elementary charge-transfer process, one electron hops between the metal and the projectile. An initial classification of these processes can be given according to whether the transferred electron loses energy or not. If it does not, that is, if the initial and final states of the electron are degenerate in energy, the process is known as *resonant*. For an electron to be resonantly captured by a slowly moving projectile, there must be an unoccupied atomic level degenerate with an occupied metal state. In other words, the atomic level must lie below the highest occupied state in the metal. The inverse process (resonant loss) is possible when an oc-

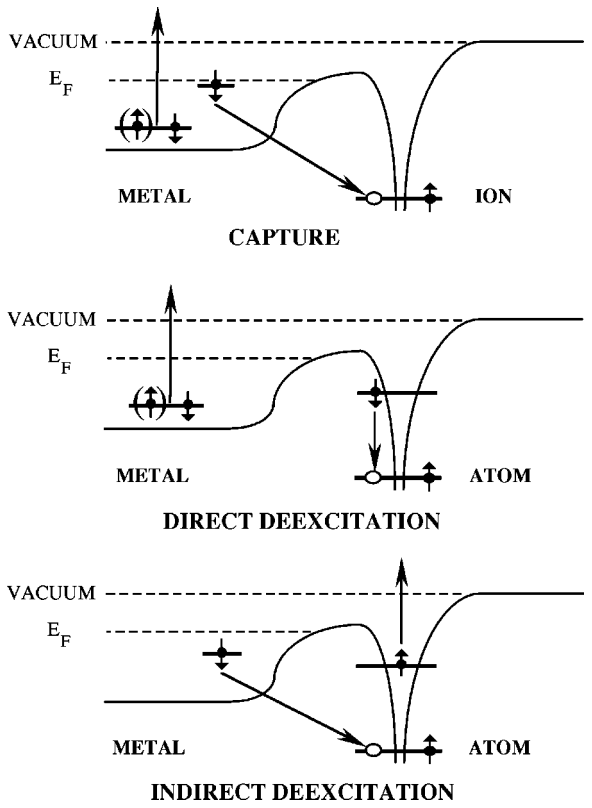

FIG. 1. Scheme of the Auger processes at a metal surface. See Sec. I for more details.

cupied atomic level is degenerate with an unoccupied metal state.

As for the processes in which the transferred electron loses energy, we shall be concerned with those known as *Auger* processes. All these processes share the common feature that an electron is captured into an unoccupied atomic level of lower energy. The energy of the transition is used for exciting either the projectile or the surface. Therefore, Auger processes can be classified according to where the captured electron was initially located and which system (surface or projectile) is excited. If the electron is captured from the metal and the surface electrons are excited, the process is called Auger *capture*, or *neutralization* when the ion is neutralized (see Fig. 1). However, if after capturing a metal electron, the projectile decays by emitting one atomic electron to the continuum, the process is termed *indirect deexcitation* (see Fig. 1). Otherwise, the electron can fill the atom core hole from an excited atomic level. In this case, there is no charge transfer between the metal and the projectile, but the energy of the transition can be given away to the metal so that a surface excitation is produced. This possibility is called *direct deexcitation* of the projectile (see Fig. 1). For completeness, we shall mention a similar process where the energy of the atomic transition excites the projectile itself. This process is well known in atomic physics, where it is called *autoionization.*

The system considered in this paper, namely, He^+ impinging on aluminum is the standard model system for Auger neutralization. The reason is that, in a collision of a slow He^+ ion with an aluminum surface, metal electrons cannot populate the ground state by resonant transfer because it is not degenerate with any metal state. Indeed, the first ionization potential of helium ($E_I = 24.6$ eV) is larger than the sum of the Fermi energy ($E_F = 12.5$ eV) and the work function ($\phi \approx 4$ eV in the jellium approximation) of aluminum. Far from the surface, the excited states of helium are degenerate with the conduction band of aluminum. At low ion velocities, however, the probability of populating the atom excited states by resonant transfer is small because the interaction with the metal shifts their energies above the Fermi level. Therefore, the Auger capture from the conduction band is expected to be the most efficient neutralization mechanism of the incoming ion. Since the capture is to the ground state, the spin of the neutralizing electron must be aligned in the opposite direction to the spin of the electron in the ion core.

Theoretical models of resonant charge transfer have successfully explained the experiments in which this mechanism is responsible for the capture of surface electrons by the impinging ion.[4] On the other hand, calculations of Auger rates have not yet achieved good agreement with the available experimental data. Experimental estimates of the most probable neutralization distance for He^+ on different targets[1,5] give values where it is expected that the perturbation of the surface-potential barrier by the ion will be very important. In the present approach, we have introduced the modification in the wave function of the captured electron caused by the ion. This represents an improvement over previous approaches, which have either neglected or treated in an approximate way this effect (see Sec. II). The distorsion of the metal wave function induced by the presence of the ion is expected to increase the electron density around the ion and thus yield a larger Auger neutralization rate. Indeed, earlier works on this effect[6] have found a substantial increase of the neutralization rate. One of the aims of the present work is to investigate this effect on the Auger process when the ion perturbation is fully taken into account. Here, we define the state of the captured electron as an eigenstate of a one-electron Hamiltonian for the ion + surface system. Therefore, it will be *a priori* a mixture of atomic and metal states. As a result, the separation between the Auger neutralization and the Auger *direct* deexcitation is not as sharp as stated above.[7] The initial states for these processes are mixed whereas the final states are identical. Indeed, they correspond to two different experimental situations: the neutralization of a He^+ ion or the deexcitation of an excited helium atom (He*). We show below the results of this unified treatment of the two processes and how the rates can be obtained independently. A preliminary account of the work presented here can be found in Ref. 7.

This paper is organized as follows. Section II contains a brief overview of the different theoretical approaches to the problem of Auger neutralization. In Sec. III, we present the formalism used in the calculation as well as the approximations involved. The details of the calculation are also reported there. Results will be found in Sec. IV. Their discussion appears in Sec. V. The main conclusions of this work can be read in Sec. VI.

II. OVERVIEW

This section contains a brief overview on the Auger processes taking place near metal surfaces. The surface Auger

processes, although related to those occurring in bulk, have intrinsic characteristics and difficulties that make them different. Hence, in this overview we will be concerned with the Auger processes at surfaces as described in the Introduction.

When looking in the literature one realizes that calculations evaluating the neutralization of ions are difficult and open to new developments. However, it has been subjected to intense research ever since the theoretical work by Massey[8] and Shekhter[9] who first calculated Auger transition rates.

In the 1950s, the work by Hagstrum[1] settled down the basis of both experimental and theoretical treatments of the surface Auger transitions. He used the energy spectrum of emitted electrons to determine fundamental properties of the ion-surface system. He was able to extract from his experimental data the neutralization distance of He^+ ions scattered off various metal surfaces by taking into account the energy balance of the emitted electrons. His work also defined the basic ingredients for a complete theoretical description of Auger neutralization. However, due to the difficulty of the required computations, his theoretical results were only qualitative.

Recent experimental work can be divided into two types of experiments: electron spectroscopy[10–14] and ion spectroscopy.[15–20] The first type deals with the energy distribution of the electrons collected during the collision of very slow ions with metal surfaces, and the second type deals with the charge state of the particles reflected from the solid surface. Very accurate measurements by Winter[20] can resolve the angular dependence of the scattered particles in very grazing collisions. From the width of the ion angular distribution, and its shift relative to the specular scattering, they can relate the ion-surface attraction to the region of neutralization, and hence obtain the distance of neutralization and approximate neutralization rates.[5]

In an analogous way, the theoretical work can also be divided into calculations concerning electron emission,[21–26] or neutralization rates.[27–35] Propst[21] calculated the Auger matrix elements using a WKB approach for the wave function of the captured electron tunneling through the ion-surface barrier. His work qualitatively reproduces the experimental spectra by Hagstrum.[1] He estimated that about 50% of the emitted electrons were not directly emitted by the Auger process but were coming from secondary electron-electron collisions inside the solid. Later on, Appelbaum and Hamann[22] computed the electron emission spectra for a silicon surface. Their calculation basically consisted in convoluting the local density of states of an electron around the ion, with the local density of states of a subsurface electron. The idea behind this approximation is that the neutralizing electron is somehow captured from the ion surroundings, whereas the emitted electron comes from the subsurface region. It is also interesting to mention the qualitative approach to the theory of Auger neutralization presented by Heine.[36] He showed that the emitted electron is a strong signature of the electronic structure of the first surface atomic layer.

Other calculations trying to extract information about the surface electronic structure from the emission spectra are the ones by Hood *et al.*,[23] and Modinos and Easa.[24] The main difference of these two approaches lies in the interpretation of which part of the electronic density of states gives the largest contribution to the emission spectra.

A different approach is taken in Refs. 6 and 25. There, the emphasis is placed upon the screening of the electron-electron interaction, while using the density of states corresponding to a free-electron-like metal (s-p bands). It is studied how this affects the measured spectra of emitted electrons. In these two articles, the dynamics of the ion-surface interaction is accounted for by computing the neutralization rate and using rate equations to follow the evolution of the different ion charge states.

The neutralization rate is a rich quantity because it gives direct information on the likelihood of a given process. It can be used in a rate equation[1,37] to obtain the ion population at a given distance from the surface. Any realistic account of the emission spectra should include the dynamical process of electron emission along the ion trajectory. In a semiclassical way, the neutralization rate takes care of this. However, not only is the neutralization rate important in this way. In Ref. 6 it is shown how the calculation of the rate is intrinsically related to the calculation of the contribution to the electron spectra.

Both Massey[8] and Shekhter[9] calculated transition rates. These are complex quantum-mechanical scattering calculations, where many approximations are required. Horiguchi *et al.*[27] and Hentschke *et al.*[28] computed Auger rates for a proton-metal system using analytical wave functions for the metal electrons (those of a step potential). They simplified the eight dimensional k-space integration by taking the contribution of electrons at the Fermi level normal to the surface. Janev and Nedeljković[29] reduced the phase space of integration drastically and considered only the dipolar term of the electron-electron interaction, thus obtaining analytical expressions for the Auger rates. In a more recent paper, Mišković and Janev[38] included the ion motion in the Auger neutralization rates by using the simplifying assumption that the matrix elements are isotropic in k space. Zimny *et al.*[31] pursued this approach and included a ''universal'' function of the ion velocity and the atomic level, taking into account all the behavior of the Auger rate with the ion motion.

The effect of parallel velocity on the Auger neutralization of ions under glancing incidence conditions and the effect of the corrugation of the solid surface has also been studied by Kaji *et al.*[37,39] They used simplified electron wave functions and treated the electron interaction in the (linearized) Thomas-Fermi approximation. Besides these approximations, they included further simplifications of the matrix elements in order to have a tractable theory. Simplified wave functions and the same screened interaction were used by Wille[40] in his study of Auger neutralization of highly charged ions. He studied the dependence of the Auger neutralization rate on arbitrary atomic quantum numbers and ion-surface distance.

Many of the above approaches describe the screening of the electron-electron interaction in the Thomas-Fermi approximation. Fondén and Zwartkruis[33] showed that the Auger rate strongly depends on the Thomas-Fermi *screening length* λ_{TF}, and thus this could lead to unphysical results because of the difficulty of defining λ_{TF} in the selvedge of the solid. Unlike most of the authors cited above, Fondén and Zwartkruis[33] used accurate numerical local-density ap-

proximation (LDA) wave functions to describe the metal electrons. Then, they evaluated the neutralization rate in the first Born approximation (or equivalently, using Fermi's golden rule as in the present case). They computed the multidimensional integrals with Monte Carlo techniques, and used the unscreened Coulomb interaction between two electrons. However, Lorente and Monreal[35] showed that the use of the unscreened Coulomb potential leads to an incorrect description of the electron-hole pair excitation at the metal surface during the neutralization process. The systems analyzed in most of these works imply energy transfers near the metal plasma frequency. Unscreened interactions may be correct for energy transfers well above the plasma frequency.[35,36] Lorente and Monreal used LDA wave functions and a full dynamically screened interaction, presenting a thorough analysis of the surface metal response during the ion neutralization. In this way, they were able to account for the possibility of plasmon excitation by the neutralizing electron. The neutralization of ions assisted by plasmon excitation has been considered in both homogeneous systems[41] and surfaces.[30,34] The work of Lorente and Monreal[35] is the surface generalization in the LDA formalism of the bulk treatment by Guinea *et al.*[41] In contrast to Refs. 30 and 34, where only the plasmon excitation is considered, in Ref. 35, the whole spectra of surface electronic excitations is included.

Despite all these theoretical efforts, serious discrepancies of several orders of magnitude are still found between the theoretical rates and the experimentally estimated ones.[1,5,11] All of the above approaches use wave functions for the metal and atom states that are defined independently and are coupled via the electron-electron interaction. This is not correct because the ion potential itself is not a negligible perturbation for the metal electrons. References 6, 32, and 33 considered this effect. The first two works used a one-dimensional ion-surface barrier to estimate the enhancement of the transition rate caused by the perturbation of the surface-potential barrier. Their conclusion is that the neutralization rate changes by orders of magnitude, shifting several atomic units into the vacuum the typical Auger neutralization distance. Schins *et al.*[32] evaluated the effect of the ion potential on the neutralizing electron wave function by using a modified second-order perturbation rate, where the intermediate states included atomic states, and also concluded on the importance of the effect of the ion potential on the electron wave function.

One of the aims of the present paper is to calculate Auger neutralization rates with the appropriate initial and final electron wave functions taking into account the ion+surface potential.

III. THEORY

A. Formalism and approximations

The usual approach to calculate the rate of Auger neutralization begins with Fermi's golden rule. To first order in perturbation theory, the probability per unit time for the ion to be neutralized by a metal electron of quantum numbers labeled by k is[35]

$$\Gamma_k=\frac{2\pi}{\hbar}\int_0^\infty\frac{d\omega}{\pi}\int\frac{d^2\mathbf{q}}{(2\pi)^2}\int dz\int dz'\,\mathrm{Im}[-\chi(q,z,z',\omega)]\times A_{sk}^*(\mathbf{q},z)A_{sk}(\mathbf{q},z')\,\delta\left(\omega-\frac{E}{\hbar}+\frac{E_s}{\hbar}\right),\tag{1}$$

where

$$A_{sk}(\mathbf{q},z)=\left\langle s\left|\frac{-2\pi e}{q}e^{-q|\hat{z}-z|}e^{i\mathbf{q}\cdot\hat{\mathbf{x}}}\right|k\right\rangle,\tag{2}$$

is called Auger matrix element.[40] We have used the following notation: z denotes the coordinate normal to the surface so that $\mathbf{r}=(\mathbf{x},z)$ is the position vector of the electron; $\mathbf{x}=(x,y)$ and the wave vector $\mathbf{q}=(q_x,q_y)$ lie on the surface plane. Notice that the quantity $(2\pi/q)e^{-q|\hat{z}-z|}e^{i\mathbf{q}\cdot\hat{\mathbf{x}}}$ is nothing but the two-dimensional Fourier transform of the Coulomb potential. This allows us to interpret the Auger matrix element as the electric potential generated by a charge distribution given by $(-e)\phi_s^*(\mathbf{r})\phi_k(\mathbf{r})$,[42] where $\phi_k(\mathbf{r})=\langle\mathbf{r}|k\rangle$ and $\phi_s(\mathbf{r})=\langle\mathbf{r}|s\rangle$ define the initial and final states of the neutralizing electron, respectively, and E and E_s the corresponding energies. The states $|k\rangle$ and $|s\rangle$ are solutions of the Schrödinger equation for one electron interacting with the ion + surface system, where the ion is placed in front of the surface at a fixed distance Z. $|s\rangle$ represents an electron bound in the ground state of the helium atom and $|k\rangle$ corresponds to a state of higher energy, which can be more or less localized in the metal. This is because the presence of the ion affects the metal electrons by attracting them, leading to the mixing of the atomic levels with the conduction-band states.

Besides the Auger matrix element, a second ingredient in Eq. (1) is the response function, $\chi(q,z,z',\omega)$, which describes how the surface responds to a weak electric field. From a quantum-mechanical point of view, an external field excites the system. Since the lowest excited states of the system can be described in terms of elementary excitations,[43] the response function contains information about the spectrum of excitations. Indeed, the imaginary part of the response function gives the probability to create an elementary excitation of energy ω and parallel momentum q.[44] In other words, it gives the spectral weight of the excitation.

The same equation can be applied to compute either the neutralization rate or the *direct* deexcitation rate. The Auger neutralization corresponds to the case where $\phi_k(\mathbf{r})$ represents a metal electron, whereas the *direct* deexcitation process corresponds to the case where it represents an electron in an excited atomic state. In our approach, however, the states $\phi_k(\mathbf{r})$ are the eigenfunctions of the ion + surface system and thus correspond to a mixture of metallic and atomic levels. In this way, the neutralization and deexcitation processes appear to be mixed. In Secs. IV and V, we will come back to this issue. In the present section, we only consider the neutralization process, i.e., we assume that ϕ_k has a dominant metal character. The total neutralization rate is obtained by summing the partial rate given by Eq. (1) over all occupied metal states,

$$\Gamma=\sum_{k\ occupied}\Gamma_k.\tag{3}$$

The interpretation of Eq. (1) is simple: The captured electron gives rise to an electric field that excites the surface. The product $A^*_{sk}(\mathbf{q},z)A_{sk}(\mathbf{q},z')$ is the probability for an electron in a state $|k\rangle$ to make a transition to the state $|s\rangle$, with a transfer of parallel momentum equal to $\hbar\mathbf{q}$ and energy $\hbar\omega = E - E_s$. This probability must be multiplied by the probability to create a surface excitation of the same energy and momentum, given by (minus) the imaginary part of the response function.[44]

However, despite this simple interpretation, Eq. (1) involves a certain number of approximations. First, it is assumed that the captured electron comes from the conduction band. These are the most energetic electrons in the metal. Therefore, they penetrate farther into the vacuum and are more likely captured by the incoming ion. Moreover, since conduction electrons in aluminum interact weakly with the crystal lattice, we can use the jellium model to describe the metal.

The jellium model is translationally invariant in the directions parallel to the surface. As a consequence, the parallel momentum must be conserved. However, putting an ion in front of the surface breaks the translational invariance of the system so that the parallel momentum is no longer a good quantum number. This means that the states $|k\rangle$ are not labeled by $\mathbf{k}=(k_x,k_y)$ anymore, but by a different set of quantum numbers (see below).

In the energy range given by the transition energy in the Auger neutralization of helium at an aluminum surface (up to $E_I - \phi = 16.6$ eV), the response of the surface can be described by the response of the conduction electrons. Thus, interband transitions as well as other types of nonelectronic excitations (phonons, etc.) can be neglected. Due to translational invariance, the excitations of an unperturbed jellium surface have well-defined parallel momentum $\mathbf{q}$. These excitations can be then classified in electron-hole pairs and plasmons. The former have a continuous energy spectrum whereas the latter are collective modes of the system with well-defined energies. For a planar surface, two types of collective modes exist: Bulk plasmons,[44] whose characteristic frequency (in the long wavelength limit) is $\omega_p = \sqrt{4\pi e^2/m n_0}$ and surface plasmons.[45] The typical energy of the (monopolar) surface plasmon is $\hbar\omega_s = \hbar\omega_p/\sqrt{2}$ as $q \to 0$. The presence of the ion in front of the surface will *a priori* modify the spectrum of excitations. Since the imaginary part of the response function describes the structure of this spectrum, to evaluate the neutralization rate we should, in principle, compute the response of the ion + surface system. However, it is expected that the effect of the presence of the He^+ on the surface response function is of order $1/N$, where N is the total number of electrons. Moreover, in the neutralization or *direct* deexcitation processes, only the metal electrons are excited. For the system considered here, the transition energies are small enough for the response of the metal to be dominated by the conduction electrons. The excitations of the system are extended over the whole surface and it seems then reasonable to approximate the response of the ion + surface system by the response of the unperturbed jellium surface. This has the drawback of neglecting the excitations of the electrons bound to the ion. This type of excitations is produced in an *indirect* deexcitation process, for example (see Fig. 1), which cannot be studied using Eq. (1).

The main approximation in Eq. (1) is the assumption that the captured electron can be distinguished from the rest of the metal electrons. Indeed, it is treated as an external particle that modifies its inner state giving rise to the electric potential $A_{sk}(\mathbf{q},z)$. This approximation is tantamount to neglecting the quantum-mechanical interference with all the exchange processes, which correspond to interchanging the final states of the electrons involved in the capture process. These include both the neutralizing electron and the metal electrons participating in the excitation. Actually, as far as the captured electron is concerned, the formalism used in this work relies on the independent electron approximation. The eigenfunctions $\phi_k(\mathbf{r})$ are obtained by solving a one-electron Schrödinger equation for the ion+surface system assuming that the captured electron moves in an effective potential, $V_{ion+surf}$, which represents a helium ion in front of a metal surface. This treatment singles out the captured electron from the beginning and thus treats it as an independent particle. However, it must be remarked that this is not so for the electrons involved in the surface excitation, which are collectively described by the response function. This function has been evaluated self-consistently in order to include the many-body aspects of the response of an electron gas. It can be expected that the error at large ion-surface distances in neglecting exchange will be larger in the case of neutralization than in the case of de-excitation. In the latter case, the exchange process involves an electron transfer and is then less likely at large ion-surface distances. For the neutralization process, the error due to neglecting exchange can be estimated from the work by Salmi[25] to be around 20% of the total neutralization rate.[35]

Finally, Eq. (1) is strictly valid when the velocity of the ion (v) is zero. However, it can still be used when v is much lower than the Fermi velocity v_F. If this condition is fulfilled, the adiabatic approximation allows us to neglect the effect of the motion of the ion on the neutralization rate. The first consequence of this approximation concerns the calculation of the wave functions $\phi_k(\mathbf{r})$. Let us write $V_{ion+surf}$ as

$$V_{ion+surf} = V_{ion} + V_{surf} + V_{ind}, \tag{4}$$

where V_{ion} is the potential of the isolated ion, and V_{surf} is the potential of the unperturbed jellium surface. The additional term V_{ind} is due to the charge induced by the ion on the surface. If the ion is moving, V_{ind} will be time dependent. In the adiabatic approximation, the time dependence of V_{ind} is neglected, and it is calculated as if the ion were fixed at a given distance from the surface. Moreover, in the reference frame of the ion the energy of a surface excitation carrying parallel momentum $\hbar\mathbf{q}$ appears to be shifted by an amount equal to $\hbar\mathbf{q}\cdot\mathbf{v}_\parallel$, where $\mathbf{v}_\parallel$ is the component of the ion velocity parallel to the surface. This is known as Doppler shift and can be neglected if $\hbar\mathbf{q}\cdot\mathbf{v}_\parallel$ is small compared to the typical excitation energy, which is in the order of the Fermi energy E_F. Since $\hbar q \sim m v_F$ typically, the Doppler shift will be negligible when $v_\parallel \ll v_F$.

B. Details of the calculation

As we have mentioned above, the Auger matrix element has to be calculated using the eigenfunctions of the Hamiltonian for the ion + surface system, which define the initial

and final states of the captured electron. They are solutions of the following Schrödinger equation:

$$\frac{-\hbar^2}{2m}\nabla^2\phi_k(\mathbf{r})+V_{ion+surf}(\mathbf{r},Z)\phi_k(\mathbf{r})=E\phi_k(\mathbf{r}). \quad (5)$$

In principle, the potential created by the ion in front of the metal surface $V_{ion+surf}$ should be computed self-consistently. However, a local-density approximation (LDA) calculation would not yield the correct image shift for the atomic excited states. Instead, we have used a model potential that reproduces the most relevant features of a self-consistently calculated $V_{ion+surf}$. With the separation of $V_{ion+surf}$ given by Eq. (4) as a starting point, we have used the parametrization from Ref. 46 for V_{surf}. This parametrization interpolates between the LDA Kohn-Lang potential close to the surface and the image potential $-e^2/4z$ at large distances. For V_{ion}, the model potential given in Ref. 47 has been used. It accurately reproduces the experimental values of the excitation energies of the singlet helium atom. Finally, V_{ind} has been approximated by the classical image potential,

$$V_{ind}(\mathbf{x},z)=\begin{cases}\dfrac{e^2}{\sqrt{\mathbf{x}^2+(z+2Z)^2}} & \text{if } z>-Z\\ -V_{ion}(\mathbf{x},z) & \text{if } z\leqslant -Z,\end{cases} \quad (6)$$

where the origin has been set at the ion nucleus so that the image reference plane lies at $z=-Z$ and the image charge is located at $\mathbf{r}=(0,0,-2Z)$. As in the previous section, $\mathbf{x}=(x,y)$ stands for the electron position vector on a plane parallel to the surface and z is the distance to the origin in the direction perpendicular to the surface. V_{ind} changes depending on whether the electron is above or below the image plane. This is because we have assumed that the ion potential is completely screened inside the metal. This should provide a good approximation to the potential induced by the ion if the ion-surface distance Z is large. However, when $Z\sim 1a_0$, we should expect important deviations from Eq. (6).

To solve Eq. (5), we have used the coupled-angular-mode (CAM) method.[48] In this nonperturbative technique, the Schrödinger equation is solved numerically. This technique has been extensively used to calculate the energy shifts and linewidths of atomic levels interacting with metal surfaces and has been successfully applied to the problem of resonant charge transfer.[4]

For a set of energy values within the conduction band, we have computed the corresponding wave functions by solving Eq. (5). Since the model is invariant under any rotation around the ion-surface axis (OZ), the projection of the angular momentum on this axis L_z is equal to $M\hbar$, with $M=\ldots,-2,-1,0,1,\ldots$. In the CAM method, the wave function of the captured electron is expanded over a basis of spherical harmonics centered on the ion nucleus,

$$\phi_k^M(\mathbf{r})=\sum_{L\geqslant|M|}\frac{F_M^{E,L}(r)}{r}Y_M^L(\Omega_{\hat{\mathbf{r}}}), \quad (7)$$

where we have taken into account that M is a good quantum number that can be used to label the state of the electron. When the latter expansion is brought into Eq. (5), it yields a set of coupled equations for $F_M^{E,L}(r)$ since the potential $V_{ion+surf}$ is not spherically symmetric, and the different terms

$$[V_{ion+surf}]_M^{L,L'}(r)=\int d\Omega_{\hat{\mathbf{r}}}Y_M^L(\Omega_{\hat{\mathbf{r}}})^*\times V_{ion+surf}(r,\theta)Y_M^{L'}(\Omega_{\hat{\mathbf{r}}}) \quad (8)$$

couple the different L components. When this set of coupled equations is solved for each E and M, it turns out that, as $r\to\infty$, the $F_M^{E,L}(r)$ remain coupled because not all the $[V_{ion+surf}]_M^{L,L'}(r)$ vanish infinitely far from the ion. The diagonalization of the potential matrix $[V_{ion+surf}]_M^{L,L'}(r)$ yields a new basis set of angular modes $X_M^n(\Omega_{\hat{\mathbf{r}}})$, known as adiabatic basis. A transformation into this new basis defines a new set of radial wave functions such that

$$\phi_k^M(\mathbf{r})=\sum_n\frac{G_M^{E,n}(r)}{r}X_M^n(\Omega_{\hat{\mathbf{r}}}). \quad (9)$$

If we truncate the expansion (7) at given value of $L=L_{max}+M$, we have for a given value of the energy E, only L_0 open *channels*. From the asymptotic behavior of $G_M^{E,n}(r)$, we can extract the scattering $S_M^n(k)$ matrix and construct a complete basis set that spans the space of open channels, whose dimension is L_0. These states are labeled by the E, M, and n, and are written as

$$e^{iM\varphi}\psi_M^{E,n}(|\mathbf{x}|,z). \quad (10)$$

The CAM method allows us to solve only the scattering problem of the metal electrons with the $V_{ion+surf}$ potential, we cannot use it to get the bound state $|s\rangle$. However, as we have remarked in the Introduction, the ground state of helium lies several electronvolts below the bottom of the conduction band. We can therefore expect that the hybridization of this level with the conduction band will be negligible, and the wave function $\phi_s(\mathbf{r})$ that describes an electron bound in the ground state of helium in front of the surface will retain a strong atomic character. In other words, to calculate this wave function, the potentials V_{surf} and V_{ind} can be safely neglected. We have solved the Schrödinger equation for an electron moving in V_{ion} variationally. We used a function of the form

$$\phi_s(r)=\frac{a_0^{-3/2}}{\sqrt{4\pi}}(A\,e^{-\alpha r}+B\,e^{-\beta r}+C\,e^{-\gamma r}). \quad (11)$$

The lowest energy is attained for $A=0.505$, $B=1.644$, $C=2.347$, and $\alpha=1.003a_0^{-1}$, $\beta=4.459a_0^{-1}$, $\gamma=1.409a_0^{-1}$. Given this parametrization, the exact numerical solution is fitted within less than one per cent error in a $5a_0$ radius around the nucleus. Moreover, it compares fairly well with the fit of the Hartree-Fock solution provided by Bransden and Joachain,[49] $\phi_s(r)$ being slightly more extended. Following this procedure, we get an eigenfunction of Eq. (5) as $Z\to\infty$, but not when Z is finite. As a consequence, $\phi_s(r)$ is not completely orthogonal to the $\phi_k(\mathbf{r})$ calculated with the CAM method. In the calculation of the Auger rate, the $\phi_k(\mathbf{r})$ functions have therefore to be orthogonalized to $\phi_s(r)$, al-

though they overlap very little. To check the validity of our choice of $\phi_s(r)$, we have performed a variational calculation of the $\phi_s(\mathbf{r})$ using the total potential $V_{ion+surf}$. We found that, by adding a term of the form $zf(r)$ to the function $\phi_s(r)$ given by Eq. (11), the lowest energy was obtained when the coefficient of the added term was negligible. This means that $\phi_s(\mathbf{r})$ is a good approximation to the full ion +surface eigenstate at the bound-state energy E_s. This energy is defined by the ionization potential of the helium atom in front of the aluminum surface, which is not just the ionization potential of the isolated atom E_I. Indeed, in front of a metal surface less energy is necessary to take one electron from the atom to infinity, due to the interaction with the metal. Classically, the energy shift is given by the image potential $e^2/4Z$, where Z is the distance from ion to the image plane. Thus,

$$E_s = E_I + \frac{e^2}{4Z}. \tag{12}$$

This expression, however, diverges as $Z \to 0$, and we have therefore saturated the variation of E_s with Z to 4 eV.

Introducing Eqs. (10) and (11) into the expression for the Auger matrix element Eq. (2) we obtain

$$A_s^{E,n}(M,q,z) = \frac{(-2\pi)^2 e}{q}(-i)^M \int_0^\infty d|\mathbf{x}||\mathbf{x}| J_M(q|\mathbf{x}|) \times \int_{-\infty}^{+\infty} dz' e^{-q|z'-z|} \psi_M^{E,n}(|\mathbf{x}|,z') \phi_s(|\mathbf{x}|,z'), \tag{13}$$

where $J_M(x)$ is the Bessel function of Mth order. It can be seen that the larger M is, the smaller the Auger matrix element will be. This means that the largest contributions to total neutralization rate,

$$\Gamma(Z) = \int_0^{+\infty} dE\, \theta(E_F - E) \sum_{M=-\infty}^{+\infty} \sum_n \Gamma(E,M,n), \tag{14}$$

will come from a few terms. Indeed, in Sec. IV it will be shown that the leading contribution to the total rate $\Gamma(E)$ comes from the $M=0$ and $|M|=1$ terms. We have thus found that the total Auger rate can be expanded in a series involving the contributions of the various M's, and that only the lowest ones are needed to obtain a good approximation to the rate.

We now turn our attention to the second ingredient in Eq. (1), namely, the response function. The calculation of $\chi(q,z,z',\omega)$ is not easy since electrons in the conduction band interact with each other through the long-range Coulomb potential. The application of an external electric field to a metal induces charges and currents, giving rise to a macroscopic electric field. This field is the superposition of the external perturbation and the field created by the induced charges themselves. Indeed, the way in which the induced charges are distributed depends on the total electric field. Hence, it is necessary to find the total field and the induced charge density in a self-consistent way. Let ϕ_{ext} be the externally applied electric potential, and let us define the response function of the system as

$$(-e)\,\delta n^{(1)}(\mathbf{r},\omega) = \int d^3\mathbf{r}'\chi(\mathbf{r},\mathbf{r}',\omega)\phi_{ext}(\mathbf{r}',\omega), \tag{15}$$

where $\delta n^{(1)}(\mathbf{r},\omega)$ is, to linear order in the external potential, the deviation from the ground-state electronic density $n_0(\mathbf{r})$.

In an interacting system, the Coulombic interaction introduces correlations between the electrons that cannot be easily treated. To get around this difficulty, one considers a fictitious system of independent particles moving in an average potential $v_{eff}(\mathbf{r})$. Kohn and Sham[50] showed that, under certain conditions, $v_{eff}(\mathbf{r})$ can be chosen to give the ground-state density of the interacting system. It is advantageous to study the response of this system to a perturbing potential ϕ_{scf}. In a way similar to Eq. (15), we can define

$$(-e)\,\delta n_0^{(1)}(\mathbf{r},\omega) = \int d^3\mathbf{r}'\chi_0(\mathbf{r},\mathbf{r}',\omega)\phi_{scf}(\mathbf{r}',\omega), \tag{16}$$

as the independent particle response function $\chi_0(\mathbf{r},\mathbf{r}',\omega)$. Since the particles in the fictitious system are independent of each other, that is, their motion is uncorrelated, we can write $\chi_0(\mathbf{r},\mathbf{r}',\omega)$ in terms of their wave functions and energies.[51,52] It can be shown[51,52] that there exists a potential $\phi_{scf}(\mathbf{r},\omega)$ such that $\delta n_0(\mathbf{r},\omega) = \delta n(\mathbf{r},\omega)$. The exact form of ϕ_{scf}, though, is not known and we have to resort to approximation schemes. In the random phase approximation (RPA),

$$\phi_{scf}(\mathbf{r},\omega) = \phi_{ext}(\mathbf{r},\omega) + \phi_{el}(\mathbf{r},\omega), \tag{17}$$

where

$$-\nabla^2\phi_{el}(\mathbf{r},\omega) = -4\pi e\,\delta n_0^{(1)}(\mathbf{r},\omega) \tag{18}$$

is nothing but the potential created by the induced charges. Thus,

$$\phi_{scf}(\mathbf{r},\omega) = \phi_{ext}(\mathbf{r},\omega) - \int d^3\mathbf{r}' \frac{e\,\delta n_0^{(1)}(\mathbf{r},\omega)}{|\mathbf{r}-\mathbf{r}'|}. \tag{19}$$

Using Eqs. (15) and (16), and assuming that $\delta n_0^{(1)}(\mathbf{r},\omega)$ represents a good approximation to the induced density of the interacting system $\delta n^{(1)}(\mathbf{r},\omega)$, we obtain the following equation for the response function:

$$\chi(\mathbf{r},\mathbf{r}',\omega) = \chi_0(\mathbf{r},\mathbf{r}',\omega) + \int d^3\mathbf{r}_1 \int d^3\mathbf{r}_2 \chi_0(\mathbf{r},\mathbf{r}_1,\omega) \frac{\chi(\mathbf{r}_2,\mathbf{r}',\omega)}{|\mathbf{r}_1-\mathbf{r}_2|}. \tag{20}$$

Since the jellium model is translationally invariant in the directions parallel to the surface, both χ and χ_0 depend on

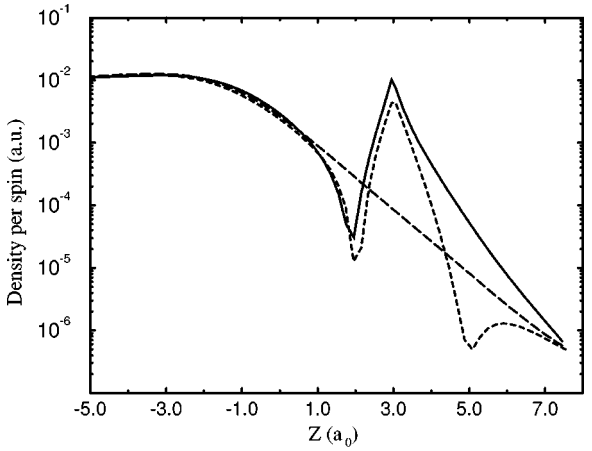

FIG. 2. Electronic density per spin state along the ion-surface axis for an ion-surface distance $Z=3a_0$, calculated using distorted wave functions $\phi_k(\mathbf{r})$ (continuous line) and orthogonalized wave functions (short dashed line) $\phi_k^{ortho}(\mathbf{r})$. The long-dashed line corresponds to the density of the unperturbed surface. All distances are referred to the image plane of the surface. See Sec. IV A for more details.

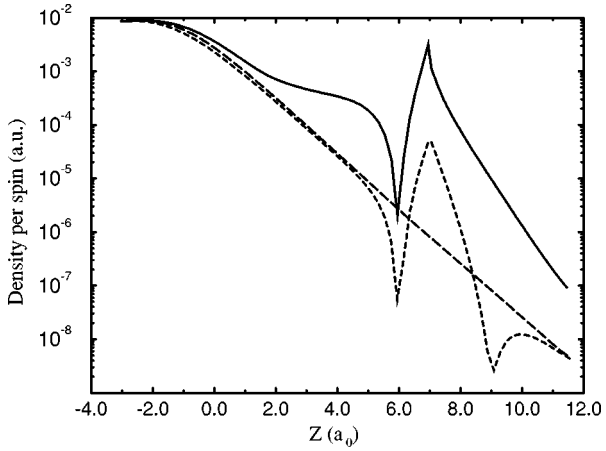

FIG. 3. Electronic density per spin state along the ion-surface axis for an ion-surface distance $Z=7a_0$, calculated using perturbed wave functions (continuous line) $\phi_k(\mathbf{r})$ and orthogonalized wave functions $\phi_k^{ortho}(\mathbf{r})$ (short-dashed line). The long-dashed line corresponds to the density of the unperturbed surface. All distances are referred to the image plane of the surface. See Sec. IV A for more details.

$|\mathbf{x}-\mathbf{x}'|$ so that it is convenient to work in Fourier space. We can write the previous equation in the following way:

$$\chi(q,z,z',\omega)=\chi_0(q,z,z',\omega) + \frac{2\pi}{q}\int dz_1 \int dz_2 \chi_0(q,z,z_1,\omega) \times e^{-q|z_1-z_2|}\chi(q,z_2,z,\omega). \quad (21)$$

This integral equation, though, is difficult to solve numerically, especially when $q \ll k_F$. In this limit, the range of the Coulomb potential becomes very long so that we have to use a large mesh in z and z' to solve the equation. Following Eguiluz and co-workers,[53,54] we have considered a jellium slab instead of a semi-infinite medium. Within the local-density approximation (LDA), the ground-state density of this system has been calculated. As a result, a set of orbitals and energies has been obtained. They have been used to construct the independent-particle response function. At this point, it seems interesting to notice that adding an image tail to the LDA surface potential has little effect on the surface response function.[55] Indeed, the surface plasmon dispersion changes very little when the asymptotic image behavior is taken into account.[55] On the other hand, such a behavior is necessary in V_{surf} when computing the captured electron wave functions $\phi_k(\mathbf{r})$. This is because it gives the right energy shift of the excited states of the helium atom.

Taking advantage of the slab geometry, the response functions $\chi_0(q,z,z',\omega)$ and $\chi(q,z,z',\omega)$ can be expanded in double cosine series. This renders Eq. (21) a matrix equation that can be solved numerically by standard techniques.[54] If the slab is thick enough, it is expected that its response function will reproduce all the features of the response of the semi-infinite jellium. We have checked that the results are independent of the slab thickness.

IV. RESULTS

A. Results for the induced electronic density

In Figs. 2 and 3, we show the effect of the ion on the electronic density. We have plotted the electronic density per spin state along the ion-surface axis for two different ion positions, $Z=3a_0$ (Fig. 2) and $Z=7a_0$ (Fig. 3) compared with that of the unperturbed surface. It is seen that the ion attracts metal electrons: the wave functions of conduction electrons are distorted and electrons pile up around the ion.

In Refs. 6 and 35, the continuum wave functions were orthogonalized to the core wave function $\phi_s(r)$. We have compared the density obtained with distorted wave functions calculated with the CAM method, with the electronic density obtained by orthogonalizing the wave functions of the unperturbed jellium surface to the atomic wave function $\phi_s(r)$ given by Eq. (11),

$$\phi_k^{ortho}(\mathbf{r})=\phi_k^{unpert}(\mathbf{r})-C_{sk}\phi_s(r), \quad (22)$$

with

$$C_{sk}=\int d^3\mathbf{r}\phi_s^*(r)\phi_k^{unpert}(\mathbf{r}). \quad (23)$$

The unperturbed wave functions $\phi_k^{unpert}(\mathbf{r})$ were obtained using the CAM method to solve Eq. (5) with $V_{ion+surf}$ replaced by V_{surf}. For $Z=3a_0$ (Fig. 2), the agreement between both calculations is much better than for $Z=7a_0$ case. The difference amounts to about a factor two at the ion position when $Z=3a_0$, whereas it increases up to two orders of magnitude when $Z=7a_0$. This is tentatively attributed to the more effective screening that the ion potential undergoes close to the surface, so that the orthogonalization procedure yields results in better agreement with the electronic density obtained with the distorted wave functions. At large distances, the ion potential favors the spill out of metal electrons. Since this effect is more important at large ion-surface distances and cannot be accounted for by the orthogonalization procedure, the results obtained with the functions

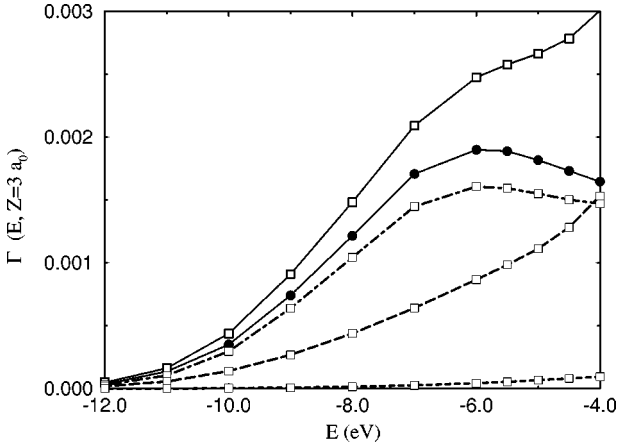

FIG. 4. Neutralization rate versus the energy of the captured electron for an ion-surface distance $Z=3a_0$. The continuous line with open squares represent the total neutralization rate obtained using distorted wave functions $\phi_k(\mathbf{r})$. The full circles is the total neutralization rate calculated with orthogonalized wave functions $\phi_k^{ortho(\mathbf{r})}$. The dot-dashed line with open squares corresponds to the $M=0$ contribution to the perturbed rate, the long dashed with open squares to twice the $M=1$ contribution, and the short dashed with open squares to twice the $M=2$ contribution. See Sec. IV B for more details.

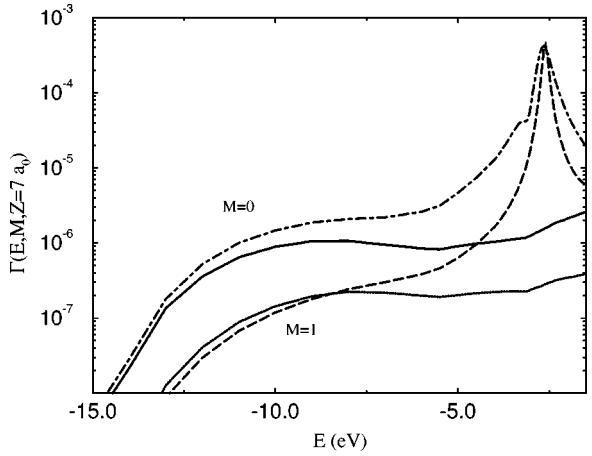

FIG. 5. Neutralization rate versus the energy of the captured electron for $Z=7a_0$. The two continuous lines represent the contribution to the neutralization rate for $M=0$ and $|M|=1$ obtained using orthogonalized wave functions, $\phi_k^{ortho}(\mathbf{r})$. The dot-dashed line is the $M=0$ contribution to the rate obtained using distorted wave functions $\phi_k(\mathbf{r})$ and the $|M|=1$ contribution is represented by the dashed line. See Sec. IV B for more details.

$\phi_k^{ortho}(\mathbf{r})$ of Eq. (22) deviate considerably from the electronic density obtained using distored wave functions, at large Z.

The convergence of the calculation with the maximum number of spherical harmonics in the CAM calculation $L_{max}+1$ has been illustrated in these figures as well. The long-dashed line represents the electronic density in the absence of the ion with $L_{max}+1=16$. The electronic densities obtained in the presence of the ion with $L_{max}+1=8$ should join the unperturbed one inside the metal. On Fig. 2, one can see that this is so for $Z=3a_0$ and some deviation is found for $Z=7a_0$ (Fig. 3), thus illustrating the effect of truncating the expansion (7) to $L_{max}+1=8$. This expansion is well-suited to describe the wave functions around the ion. However, trying to describe the electronic density far from the ion using a few L's fails to give good results. Fortunately, the leading contribution to the Auger matrix elements comes from a small region around the ion nucleus of the order of the bound-state extension, that is, a few times the Bohr radius. Therefore, we have achieved good convergence for the Auger rate with a rather limited number of spherical harmonics. The results for the Auger rate shown below were obtained with $L_{max}+1=8$.

B. The rate as a function of the energy of the captured electron. Expansion in M

Figure 4 presents the calculated neutralization rate when $Z=3a_0$ as a function of the energy of the captured electron (E, referred to the vacuum level), which ranges from the bottom of the band (-16.5 eV) to the Fermi level, taken as -4 eV in the present study. We have plotted the total neutralization rate (open squares and continuous line) as well as the different contributions of the different values of M quantum number ($M=0$ open squares dot-dashed line, twice $M=1$ open squares and long-dashed line, and twice $M=2$ open squares and short-dashed line). The total rate is

$$\Gamma(E)=\Gamma(E,M=0)+2\times\Gamma(E,|M|=1)+2\times\Gamma(E,|M|=2)+\cdots. \tag{24}$$

As mentioned above, the neutralization rate decreases rapidly with increasing $|M|$. Figure 4 shows that the expansion (24) actually converges with a few terms. Indeed, the contribution of $M=2$ to the total neutralization rate is almost negligible when compared with that of $|M|=1$ or $M=0$. We have also plotted the total neutralization rate obtained from the orthogonalized wave functions $\phi_k^{ortho}(\mathbf{r})$ (full circles, continuous line). As expected, the attraction of metal electrons towards the ion results in an increase of the Auger neutralization rate. This enhancement is particularly strong for the electrons around the Fermi level. Near the bottom of the band, the small change in $\Gamma(E,M)$ is explained by the strong metallic character that the electron wave functions have in this energy range. However, as the energy E is increased, the electrons spill out farther into the vacuum so that they feel more strongly the ion potential. The enhancement around the Fermi level is not only due to contribution of the $|M|=1$ as could be inferred by looking at Fig. 4. To show this, we have plotted $\Gamma(E,M=0)$ in Fig. 5 (dashed-dotted line) and (twice) $\Gamma(E,M=1)$, for $Z=7a_0$. We have also plotted the corresponding results obtained from the orthogonalized wave functions. It can be seen that both $M=0$ and $M=1$ contributions are enhanced by the effect of the ion onto the high energy region.

C. Structure of $\Gamma(E,M)$ above the Fermi level. Rates for the Auger direct deexcitation process

The enhancement in the neutralization rate around the Fermi level can be understood in a different way by plotting $\Gamma(E,M)$ for a wider range of energies that includes the unoccupied part of the conduction band. This is shown in Figs.

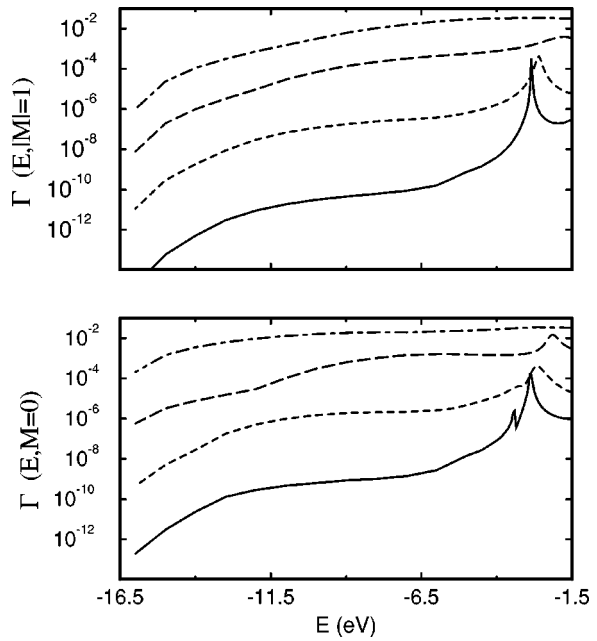

FIG. 6. Neutralization rate versus the energy of the captured electron for the ion-surface distances $Z=11a_0$ (continuous line), $Z=7a_0$ (short-dashed line), $Z=3a_0$ (long-dashed line), $Z=-1a_0$ (dot-dashed line). The graph on top is the $M=0$ contribution to the neutralization, and the graph below is the $|M|=1$ contribution. See Sec. IV C for more details.

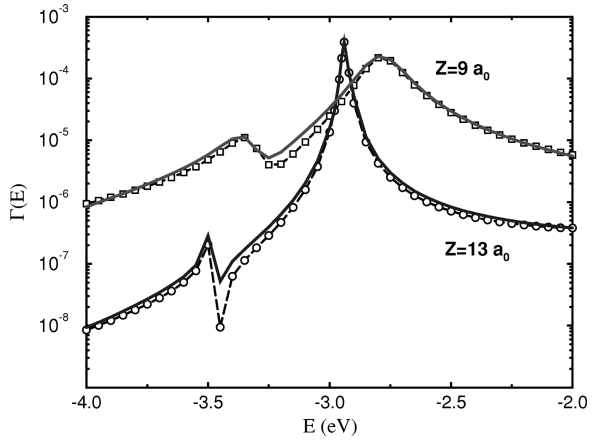

FIG. 7. $M=0$ contribution to the neutralization rate versus the energy of the captured electron, for the ion-surface distances $Z=13a_0$ (open squares) and $Z=9a_0$ (open circles) around the $n=2$ peak structure. The fit is the continuous line in both cases. See Sec. IV C for more details.

5 and 6, where we show $\Gamma(E,M)$ for $M=0$ and $|M|=1$ for different values of the ion-image plane distance $Z=11,7,3,-1a_0$. For $M=0$, a double peak structure appears at the largest distance, $Z=11a_0$. It corresponds to the 2^1S and $2^1P_{M=0}$ atomic states, which, through the interaction with the conduction band of the metal, acquire a finite width (corresponding to the resonant loss between the surface and the He excited states). The 2^1S and $2^1P_{M=0}$ levels also interact together either directly or indirectly via the coupling with conduction band.[56–58] As the ion is placed closer to the surface, the two peaks get broader and shift towards higher energies; they even coalesce for a certain distance,[57] so that below $7a_0$ from the image plane they cannot be resolved. For $|M|=1$ only one peak can be seen, corresponding to the $2^1P_{M=\pm1}$ state. Although not shown in this figure, the whole Rydberg series of the singlet excited states becomes a series of resonances due to the perturbation induced by the surface. The hybridization of the atomic levels with the metal conduction band gives some atomic character to the electron wave functions $\phi_k(\mathbf{r})$. This mixing of atom and metal states cannot be described by orthogonalizing the unperturbed wave functions to the final atomic state $\phi_s(r)$. The enhancement of the neutralization rate as the energy of the neutralizing electron approaches the Fermi level can then be looked at as the effect of the *tails* of all the (singlet) excited states of the helium atom.

In the region of the peak structure, $\Gamma(E,M)$ can be represented by the interfering contributions of various atomic resonances and a nonresonant background. To check this point, we fitted to the computed rate the following expression $\Gamma(E,M=0)$

$$\Gamma(E,M=0) = \left| \frac{A_0}{(E-E_0)+i\frac{\Delta_0}{2}} + \frac{A_1}{(E-E_1)+i\frac{\Delta_1}{2}} + A_2E + A_3 \right|^2, \tag{25}$$

where A_0,A_1,A_2,A_3 are the fitting parameters. The linear term A_2E+A_3 is taken as the simplest form of background. The two Lorentzian Breit-Wigner resonances represent the contribution of the 2^1S and $2^1P_{M=0}$ atomic resonances. E_0,Δ_0 and E_1,Δ_1 are taken from the earlier calculation of the interaction of the $n=2$ manifold of He* with the metal conduction band, reported in Ref. 56. The quality of the fit is shown in Fig. 7 for $Z=9a_0$ and $Z=13a_0$. It gives confidence in the interpretation of the structures. A_0 can be determined with a great accuracy since the rate $\Gamma(E,M=0)$ is dominated by the contribution of $2^1P_{M=0}$ in that energy range. The contribution from the 2^1S appears as a Fano resonance[57] in the tail of the $2^1P_{M=0}$ peak. Being much smaller, the quality of the fit is worse and so is the accuracy in the A_1 coefficient. The defect of the fit in this region is attributed to the fact that the tail of the $2^1P_{M=0}$ resonance is not perfectly Lorentzian in that region. The widths of the resonances Δ_0 and Δ_1 provide information on the extent of the mixing between the atomic level and the conduction-band states, and thus on the disappearance of the atomic character of the level. Notice that when the projectile is very close to the surface, the hybridization between the atomic levels and the conduction band is very strong and the atomic levels are ill-defined.

At this point, we can go back to the definition of the various Auger processes presented in Sec. I. First, for electrons with energies below the Fermi level, the $\phi_k(\mathbf{r})$ wave functions have a dominant metal character, and thus the rate computed with expression (3) or (14) corresponds to the Auger neutralization, taking into account perturbation of the ion potential. For higher energies and around certain energy values, it appears (see Figs. 5, 6, and 7) that the $\Gamma(E,M)$ rate is

dominated by an atomic contribution so that $\phi_k(\mathbf{r})$ has a strong atomic character. The analysis performed above, Eq. (25), permits us to extract from $\Gamma(E,M)$ the contribution of the atomic state, and thus to be able to describe the Auger deexcitation process. In this case, the perturbation of the process introduced by the mixture of atom and metal levels as well as between the atomic states, is taken into account. Therefore, we have found that the same quantity $\Gamma(E,M)$ can be used to describe the Auger neutralization and the *direct* deexcitation processes, just by looking at different energy (E) ranges.

The *direct* deexcitation rate is obtained by integrating over the energy the Lorentzian contribution of each atomic resonance,

$$\Gamma_{AD}(M)=\int_{-\infty}^{+\infty} dE \frac{A_R}{(E-E_R)^2+\frac{\Delta_R^2}{4}}, \tag{26}$$

with A_R, E_R, and Δ_R replaced by A_0 (A_1), E_0 (E_1), and Δ_0 (Δ_1), respectively for $M=0$, or by the corresponding values for $|M|=1$. This procedure allows us to separate the various atomic contributions, and therefore to obtain the deexcitation rate for each atomic resonance with just one excited atomic electron. The procedure can only be applied when the ion is placed far from the surface (large Z values) and the atomic contributions to $\Gamma(E,M)$ can be resolved. As the atom is brought closer to the surface, the widths of the $(n=2)$ He* states become too large and the states lose their atomic character so that the deexcitation process cannot be defined anymore.

D. Total Auger neutralization and direct deexcitation rates

Finally, Figs. 8 and 9 show the total neutralization and *direct* deexcitation rates, respectively. In Fig. 8, we have compared the results obtained using distorted wave functions for the conduction-band electrons (continuous line and open squares) or unperturbed surface wave functions orthogonalized to the $\phi_s(\mathbf{r})$ atomic state (continuous line and full circles). Furthermore, we have varied the model for surface response used in the calculation. Along with the RPA response function [Eqs. (19) and (21)], we have used a different approximation for ϕ_{scf}, which consists in adding a local-field correction due to exchange and correlation. More explicitly, Eq. (17) is replaced by

$$\phi_{scf}(\mathbf{r},\omega)=\phi_{ext}(\mathbf{r},\omega)+\phi_{el}(\mathbf{r},\omega)+\phi_{xc}(\mathbf{r},\omega), \tag{27}$$

where

$$\phi_{xc}(\mathbf{r},\omega)=\frac{dV_{xc}}{dn}[n_0(z)]\delta n(\mathbf{r},\omega). \tag{28}$$

V_{xc} being the exchange and correlation part of the LDA to the $v_{eff}(z)$ potential, and $n_0(z)$ the ground-state electronic density of the unperturbed surface. This approximation, known as the adiabatic local-density approximation (ALDA),[59] yields a dispersion for the surface plasmon in better agreement with experiment.[60] However, in Fig. 8, we show that for rate calculated with orthogonalized wave functions, using the RPA (full circles) or ALDA response functions (open down triangles) leads to small differences in $\Gamma(Z)$. This is because the total neutralization rate $\Gamma(Z)$ is a rather integrated quantity of the response function. More important, however, seems the choice of the final atomic wave function $\phi_s(r)$. This point is also illustrated by Fig. 8. The

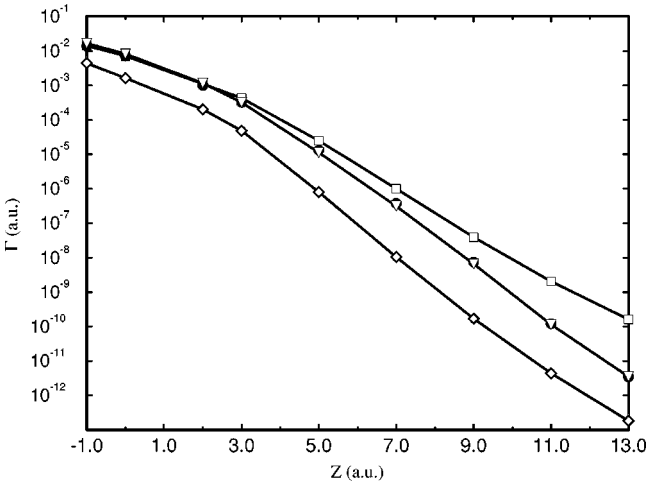

FIG. 8. Total neutralization rate versus the ion-image plane distance Z. The line with open squares represent the results obtained using wave functions for the captured electron perturbed by the presence of the ion, $\phi_k(\mathbf{r})$. Full circles correspond to the neutralization rate calculated using orthogonalized wave functions and a RPA response function whereas the open triangles refer to the same calculation using the adiabatic local-density approximation (ALDA) for the surface response function. Open diamonds correspond to the neutralization rate obtained using the unperturbed surface wave functions orthogonalized to a hydrogeniclike wave function $\phi_s(r)=(\alpha^3/\pi)^{1/2}e^{-\alpha r}$, with $\alpha=1.6875a_0^{-1}$. See Sec. IV D for more details.

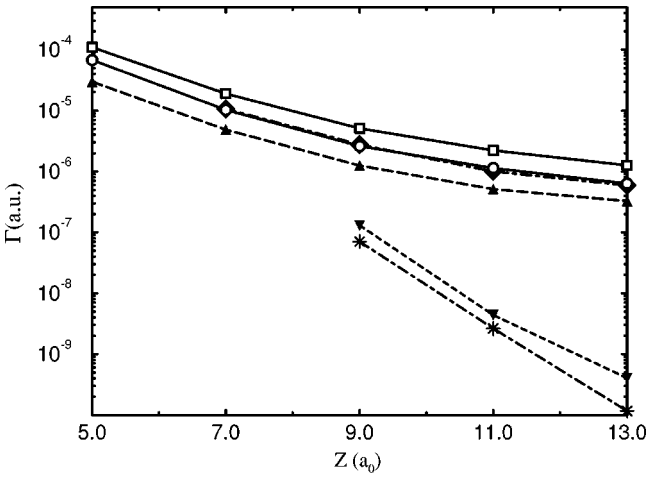

FIG. 9. Total direct deexcitation rate versus the helium-image plane distance Z. The full diamonds present the deexcitation rate for the 2^1P $(M=0)$ state with perturbed wave functions and the full up-triangles are the same results for the 2^1P $(|M|=1)$ states, respectively obtained with unperturbed atomic wave functions. The full down-triangles represent the results for the deexcitation rate of the 2^1S (*perturbed* wave function) and the stars are the results for the 2^1S deexcitation rate of the simple model based on the 2^1S-2^1P mixing via the metal continuum. See Sec. IV D for more details.

open diamonds are the results from a calculation of the unperturbed rate using the ALDA response function and a wave function of the form,

$$\phi_s'(r) = \sqrt{\frac{\alpha^3}{\pi}} e^{-\alpha r}, \tag{29}$$

where $\alpha = 1.6875 a_0^{-1}$. This value is obtained by minimizing the energy for two electrons in the ground state of the helium atom. As this wave function is more compact than the one provided by Eq. (11), we get a much smaller neutralization rate than when our first choice for $\phi_s(r)$ (open down triangles) is used. The Auger rate thus appears to be very sensitive to the description of the atom ground state, that is, of the orbital in which the metal electron is captured.

Another interesting feature of Fig. 8 is that the differences between the calculation using distorted wave functions (open squares) or the $\phi_k^{ortho}(\mathbf{r})$ of Eq. (22) (full circles) decrease as the ion approaches the surface. For instance, when $Z = 13 a_0$ from the image reference plane, the difference between the two calculations amounts to about two orders of magnitude whereas for $Z = 3 a_0$ the results are almost the same. This behavior reproduces the trends observed for the electron density in Figs. 2 and 3. The difference is very large at large Z and almost vanishes at small Z. When the ion is inside the metal, because of the complete screening assumed in our study, it is not surprising that the results obtained using distorted and orthogonalized wave functions merge (we will further elaborate on this point in next section). On the other hand, when the ion is outside the metal, the effect of the ion potential results in an increase of the neutralization rate, as expected. It is noteworthy that this increase is significantly smaller that the one found in an earlier study.[6] There, the effect of the ion was modeled by modifying the one-dimensional surface barrier. The origin of the difference between the two results rests in three-dimensional character of the ion potential. In the one-dimensional approach, the modification of the surface barrier was introduced as a potential independent of x and y, the coordinates parallel to the surface. This significantly increases the electron spill out from the surface. In contrast, in the present three-dimensional study, the surface barrier is lowered only in the vicinity of the ion; in a way, this creates a hole in the surface barrier (or rather a localized region where the barrier transparency is increased) through which the metal electrons can go. The tunneling probability of the electron in the three-dimensional problem is smaller than in the one-dimensional barrier model, in particular because of the wave character of the electron motion and this probably accounts for the difference between the one and three-dimensional effects. In addition, it must be stressed that a one-dimensional study cannot properly account for the existence of the He* states, and thus of their effect on the neutralization rate.

Figure 9 presents the results for the deexcitation rate versus the atom-surface distance (Z), as calculated following the procedure described above. We have plotted the rates for $M = 0$ (full diamonds), which corresponds to a deexcitation of the $2^1P_{M=0}$ state and for $|M| = 1$ (full up triangles), which corresponds to the deexcitation of $2^1P_{M=\pm 1}$. The full down triangles represent the deexcitation rate of the 2^1S state. We have also calculated the *direct* deexcitation rates for the unperturbed $n = 2$ states of the ion potential $V_{ion}(r)$, that is, by replacing the $\phi_k(\mathbf{r})$ wave function by the unperturbed atomic wave function in Eq. (1). The open squares are the results obtained for the deexcitation of the $2^1P_{M=0}$ atomic state, and the open circles the results for $2^1P_{M=\pm 1}$. The unperturbed results are larger than the perturbed ones because the hybridization with the conduction band is not considered. When the hybridization is taken into account, the atomic wave function loses part of its atomic character, being the electron slightly localized in the metal and thus reducing its presence in the immediate surroundings of the atom so that the deexcitation rate decreases.

The importance of the distorsion in the wave functions is seen more clearly when we evaluate the deexcitation probability of the 2^1S atomic state. In the unperturbed case, the deexcitation of the 2^1S atomic state is not possible because the matrix element, Eq. (2), vanishes when $\phi_k(\mathbf{r})$ is replaced by the 2^1S atomic orbital. Therefore, the nonzero deexcitation rate obtained when we use distorted wave functions must come from the distorsion of the atomic wave functions in the presence of the metal surface. In the following section, we shall give a more detailed discussion of this point.

Finally, we should mention that our results compare well with an independent calculation of the deexcitation rates reported in Ref. 61. In this work, a different set of atomic wave functions and a different model of the between the two calculations amounts, at most, to a factor four.

V. DISCUSSION OF THE RESULTS

As mentioned above, the assumption of complete screening of the ion potential inside the metal may raise doubts concerning the accuracy of our results for small Z values. Indeed, the problem stems from the use of a nonself-consistent potential to describe the ion + surface system. In our model, the electronic charge induced in the metal by the ion does not give rise to the V_{ind} potential when the ion is placed very close to the surface. A self-consistent potential V_{ind} would show a deviation from the classical image behavior assumed in Eq. (6). Furthermore, it would have a nonvanishing value inside the metal instead of the perfect screening that we have considered. Nevertheless, a self-consistent calculation for V_{ind} is not easily attainable. Within the framework of density-functional theory, the local-density approximation (LDA) would not yield the correct asymptotic image behavior that our model potential, Eq. (6), has. More sophisticated choices for the exchange-correlation functional involving density gradients, are likely to run into problems of numerical convergence when trying to achieve self-consistency. In bulk matter, however, the LDA is a good approximation to V_{ind} in view of its success when applied to problems as the low velocity stopping power of ions[62] or core-level spectroscopy.[63] In the following, we will show that a calculation of the rate using a self-consistent LDA potential for a He^+ ion embedded in jellium does not lead to significant differences when compared to a rate reckoned from orthogonalized wave functions. We will provide plausible arguments to show that, by neglecting the ion potential inside the metal, the neutralization rate at small Z is under-

TABLE I. Neutralization rate for He^+ in bulk aluminum ($r_s = 2.0a_0$) as a function of α [see Eq. (29)]. OLDA, orthogonalized LDA orbitals; OPW, orthogonalized plane waves.

α (a_0^{-1})	Γ_{AN} (OLDA) (a.u.)	Γ_{AN} (OPW) (a.u.)
1.4	3.98×10^{-2}	2.01×10^{-2}
1.5	3.33×10^{-2}	1.67×10^{-2}
1.6	2.77×10^{-2}	1.38×10^{-2}
2.0	1.34×10^{-2}	0.66×10^{-2}

estimated by at most a factor of two and not by orders of magnitude.

We have performed a self-consistent calculation of the neutralization rate in bulk by computing the local-density orbitals for the conduction electrons in the presence of a He^+ ion. The calculation was carried out keeping unoccupied one of the $1s$ orbitals in the atom, that is, keeping a hole in the ion core. This situation represents the ion before the neutralization has taken place and is equivalent to our surface treatment. Along with the continuum wave functions, we also obtain the wave function of the core hole, which defines the final state of the neutralizing electron. To compare with our surface results, instead of using the LDA eigenenergy for this orbital, the energy is again fixed to the same saturated E_s used above -20.6 eV. This value is only about 2 eV above the LDA result and ensures that the highest possible transition energy for both surface and bulk calculations is the same. Except for this feature, the calculation was accomplished in the same way as reported in Ref. 64. We obtain a value for the neutralization rate of 2.37×10^{-2} a.u. Using the atomic wave fuction $\phi_s(r)$ provided by Eq. (11) and the same LDA orbitals for the captured electron orthogonalized to $\phi_s(r)$, we get $\Gamma_{AN}=4.52\times10^{-2}$ a.u. This confirms the sensitivity of the Auger rate to the choice of final atomic state $|s\rangle$. Replacing the LDA orbitals by plane waves othogonalized to $\phi_s(r)$, $\Gamma_{AN}=2.24\times10^{-2}$ a.u. In addition, a calculation of the neutralization rate using a hydrogenic wave function for the core hole, Eq. (29), has been performed. We have varied the extension of the orbital, given by the parameter α. In this case, the LDA orbitals of the conduction-band electrons are not orthogonal to the core-hole wave function and have been orthogonalized to it. The results of this calculation are displayed in Table I. We have compared them to the neutralization rates obtained, in the same way, using orthogonalized plane waves instead of LDA orbitals. All these results with various atomic orbitals show that the use of orthogonalized plane waves, instead of a self-consistent description, leads to an underestimation of the Auger neutralization rate by about a factor of 2. This gives an order of magnitude for the effect of the incomplete screening of the ion potential for very small ion-surface distances. Then, we can expect the use of a model screening to have a limited effect on our results for small Z.

Now, we come back to the *direct* deexcitation issue. We have mentioned in Sec. IV that the (deexcitation) rate for the transition $2^1S\rightarrow1^1S$ must vanish unless perturbed wave functions are used. To see this, let us consider the Auger matrix element corresponding to the atomic transition in real space,

$$A(2^1S\rightarrow1^1S)(\mathbf{r})=(-e)\int d^3\mathbf{r}\frac{\phi_{2s}^*(\mathbf{r}')\phi_s(\mathbf{r}')}{|\mathbf{r}-\mathbf{r}'|}, \quad (30)$$

where $\phi_{2s}(\mathbf{r})$ stands for the wave function of the unperturbed atomic level 2^1S. As we have said in Sec. III, the Auger matrix element corresponds to the electric potential produced by the charge distribution $(-e)\phi_{2s}(\mathbf{r})\phi_s(\mathbf{r})$. This charge distribution is spherically symmetric so that *a priori* the only nonzero term of a multipolar expansion of Eq. (30) should be the monopolar $L=0$ term. This term, however, vanishes exactly since the two wave functions are orthogonal. On the other hand, we have seen above that the rate for the deexcitation $2^1S^*\rightarrow1^1S$ (where an asterisk indicates the atomic state mixed with the conduction band) is not zero. From the above analysis, this fact must come from the distorsion of the atomic orbital in the presence of the surface, that is, its mixing with the conduction-band states. Makhmetov *et al.*[56] have discussed the various state mixing occuring in the singlet spectrum of helium in front of an aluminum surface. In particular, they stressed the importance of the indirect coupling between the 2^1S and the 2^1P states taking place via the metal continuum. Following Devdariani *et al.*[58] and Makhmetov *et al.*,[56] the interaction between two discrete states and a continuum can be described by means of a Hamiltonian matrix in the subspace spanned by the two states,

$$H=\begin{pmatrix} E_1-i\frac{\Delta_1}{2} & V-\frac{i}{2}\sqrt{\Delta_1\Delta_2} \\ V-\frac{i}{2}\sqrt{\Delta_1\Delta_2} & E_2-i\frac{\Delta_2}{2} \end{pmatrix}, \quad (31)$$

where $E_1-i\Delta_1/2$ and $E_2-i\Delta_2/2$ are the complex energies of the quasionary states $|2^1S\rangle$ and $|2^1P_{M=0}\rangle$. The off-diagonal term $V-(i/2)\sqrt{\Delta_1\Delta_2}$ describes the effective interaction between the two discrete states. Whereas, V is the direct interaction between them, $(i/2)\sqrt{\Delta_1\Delta_2}$ is their interaction via the continuum.

We shall use the Hamiltonian of Eq. (31) to give a more detailed account of why the de-excitation rate of the 2^1S^* state does not vanish. First, let us notice that the presence of an imaginary part in the off-diagonal term $V-(i/2)\sqrt{\Delta_1\Delta_2}$ can result in either attraction or repulsion of the levels depending on the relative size of the real and imaginary parts of the off-diagonal term [notice that the matrix (31) is non-Hermitian]. The numerical calculations of Ref. 57 show that the levels attract, telling us that the imaginary part dominates. Therefore, for illustrative purposes, we can neglect V. Moreover, the off-diagonal term is much smaller than the difference between the diagonal term, at large Z and we can use first-order perturbation theory to evaluate the eigenstates of Eq. (31):

$$|2^1S^*\rangle=C\left(|2^1S\rangle+\frac{H_{12}}{H_{11}-H_{22}}|2^1P_{M=0}\rangle\right)+O(H_{12}^2), \quad (32)$$

where $H_{11}=E_1-i\Delta_1/2$, $H_{22}=E_2-i\Delta_2/2$, and $H_{12}=V-(i/2)\sqrt{\Delta_1\Delta_2}\simeq-(i/2)\sqrt{\Delta_1\Delta_2}$ is a shorthand for the matrix elements of H, and

$$C=\frac{1}{\sqrt{1+\dfrac{|H_{12}|^2}{|H_{11}-H_{22}|^2}}}$$

a normalization constant. Consequently, the ratio of the matrix elements of matrix (31) is roughly equal to

$$\frac{H_{12}}{(H_{11}-H_{22})}. \tag{33}$$

Hence, neglecting the small difference in the transition energies of the $2^1S^*\rightarrow 1^1S$ and $2^1P^*_{M=0}\rightarrow 1^1S$ processes (~ 1 eV), the ratio of the *direct* de-excitation rates, is equal to

$$\frac{\Gamma_{AD}(2^1S^*\rightarrow 1^1S)}{\Gamma_{AD}(2^1P^*_{M=0}\rightarrow 1^1S)}\simeq\frac{|H_{12}|^2}{|H_{11}-H_{22}|^2}\simeq\frac{\Delta_1\Delta_2}{4(E_1-E_2)^2}, \tag{34}$$

that is, the admixture coefficient. Therefore, the deexcitation rates of the two $M=0$ atomic states are not independent but closely related to each other. This relationship is due to their coupling via the continuum of conduction-band states, characterized by Δ_1 and Δ_2. We have thus shown that the deexcitation rate of the 2^1S^* state can be obtained from the knowledge of the energies and (resonant) linewidths of the two atomic resonances, and the deexcitation of the $2^1P^*_{M=0}$ state. Stars in Fig. 8 show the results of such a calculation. The agreement with the results obtained by fitting the peaks in $\Gamma(E,M=0)$ as explained in Sec. IV, is reasonably good, taking into account the approximations involved in Eq. (34). This confirms the interpretation of the 2^1S^* deexcitation rate as mainly due to the mixing of the 2^1S state with the 2^1P state.

It is interesting to compare the various rates in order to justify the use of perturbed wave functions in the computation of the Auger neutralization and deexcitation rates. Indeed, using Eq. (5) to define $\phi_k(\mathbf{r})$ assumes that the electrons had enough time to adjust to the total potential before the Auger neutralization occurs. For the Auger neutralization process, this means that the metal electrons have adjusted to the ion potential; the time required by this adjustment can be estimated from the rates for the resonant transfer (see for example the rates for the $n=2$ levels of He of Ref. 56). Since the resonant process is much faster that the Auger neutralization, the use of Eq. (5) is therefore completely justified. However, the case of the Auger deexcitation is more complex since, in the present system, the excited states are degenerate with empty metal levels. Using distorted $\phi_k(\mathbf{r})$ wave functions for the $(n=2)$ states is justified only after the electron in the excited state has been resonantly lost to the metal. Before, one should use rates computed with unperturbed atomic orbitals. Our results for the deexcitation rate (obtained using distorted wave functions) can be used only in situations where the excited state is still occupied after the resonant charge transfer has occurred. This is the case, for example, in a fast grazing collision of He^+ (or He*) on a metal surface.[5] Another situation is when the excited state is degenerate with the occupied levels of the metal conduction band. Under these conditions, the incident ion will be much faster neutralized by a resonant capture to an excited state than by an Auger capture to the ground state. After the resonant neutralization has taken place, the present approach can be used to evaluate the Auger deexcitation rate (special care has to be taken in order to ensure that the population of the excited state is equal to one). Moreover, in this case the Auger neutralization process can be disregarded except, maybe, before the resonant neutralization occurs. In the latter case, the Auger neutralization should be calculated using unperturbed wave functions.

Finally, the calculated values for the neutralization rate can be used together with a rate equation to calculate the evolution of the He^+ population.[37] The freezing distance Z^* is defined as the distance where the variation of the ion population with Z, that is, $dn_+(Z)/dZ$, is maximum. Experimental estimates[5] give a value of $Z^*=3a_0$ for aluminum. Let us consider the scattering of an ion of 2 keV of kinetic energy under glancing incidence conditions at 0.5° from the surface plane. By solving the latter equation with the neutralization rate obtained using distorted wave functions, we get $Z^*=1.5a_0$. This value is larger than in previous works,[35] $Z^*=0.5a_0$, and in better agreement with the experimental value given above. The experiments point out that the ion neutralization takes place well beyond the image plane. However, there is a considerably discrepancy concerning the distance of the image plane to the first atomic layer in the literature (see, for example, Refs. 46 and 65–67), which already gives one atomic unit of uncertitude in surface calculations. Moreover, the lack of self-consistency in the ion + surface potential may lead, as shown above, to underestimate the neutralization rate by, at most, a factor two. This translates into an uncertainty in the freezing distance smaller than one atomic unit. Therefore, we have obtained an important *qualitative* result in good agreement with experiment: the neutralization via an Auger process of slow He^+ ions takes place well beyond the image plane.

Another interesting point concerns the third Auger process depicted in Fig. 1, which has not been considered in the present work. By looking at Figs. 8 and 9, it can be seen that the probability of capturing an electron from the surface, that is, the neutralization rate, becomes larger than the *direct* deexcitation rate around $5a_0$. This suggests that below this distance, the *indirect* Auger deexcitation may become more likely than the *direct* deexcitation process considered here.

VI. SUMMARY AND CONCLUSIONS

We have calculated the rates of different Auger processes in the helium-aluminum surface system. In order to achieve this, we have studied the transition between the eigenstates of the ion+surface Hamiltonian caused by the electron-electron interaction. This approach presents fundamental differences over previous approaches.[6,35] The first feature is the inclusion of the effect of the ion potential on the surface barrier, attracting the neutralizing electrons towards the ion and increasing the Auger neutralization probabilities.

The second feature appears when applying the same formalism to Auger deexcitation rates. In the latter case, a neutral excited atom can be deexcited by filling its core while exciting the surface electronic system.

As it has been emphasized elsewhere,[35] it is of paramount

importance to include the correct surface screening in the electron-electron interaction, using in this way a theory that accounts for electron-hole pair and plasmon excitation by the captured electron. Since exchange processes are disregarded in the present treatment, we are only able to account for *direct* Auger deexcitation process. In this process, an electron in an excited state of the atom fills in the $1s$ core-hole of the atom, transferring its energy to the metal surface. The main novelty of the present calculation is that both Auger neutralization and Auger deexcitation are treated on the same footing as they correspond to particular cases of transitions between one-electron eigenstates of the ion + surface system.

The Auger neutralization rates computed with these distorted wave functions system are larger than the neutralization rates calculated neglecting the effect of the ion on the surface barrier.[35] The rate is greatly enhanced at large ion-surface distances, decreasing as the ion is brought closer to the surface.

This increase in the Auger neutralization rate induced by the ion effect can be understood in two ways. It can be related to the increase of the electronic density around the ion core (Figs. 2 and 3), or as due to the effect of the tails of the atom excited states (Figs. 5 and 6). The latter interpretation allows to discuss the importance of the effect: when an atomic state lies slightly above the Fermi level, it will strongly hybridize with the occupied metal states, leading to a significant increase of the neutralization rate. At small ion-surface distances, the excited states shift up in energy and broaden. Their effect is then more difficult to recognize, and the rate enhancement should be interpreted in the first way, namely, as due to the increase of electronic density in the ion suroundings. According to the above discussion, it seems that He^+ on Al is rather special. However, changing the projectile would modify the position of the excited levels relative to the Fermi level altering the numerical results obtained in this paper. We expect that, since the physics involved is the same, the above discussion can be equally applied.

This brings us to the second result of the present calculation: the existence of atomic excited states in front of the metal surface, which eventually can be involved in an atom core filling transition. We have been able to extract the contribution to the core-filling probability of one electron that corresponds to an excited state of the atom in front of the metal surface. Due to the metal presence, these states are strongly hybridized and even interact among themselves via the metal continuum.[56] Thus, our calculation gives the first Auger deexcitation rate in which the effect of the metal presence has been taken into account in the atomic states. The effect of the metal presence is twofold. It allows the transition because it can absorb the transition energy between the electronic states, and it distorts the atomic states. As a result, the Auger deexcitation rate is smaller when distorted 2^1P states are used, as compared to unperturbed atomic states, because the electrons spend more time away from the atom. Moreover, it allows the deexcitation of the 2^1S metastable state which is zero in a calculation where the distorsion of the atom states by the metal surface is not taken into account.[61]

A complete treatment of the Auger processes should include the *indirect* Auger deexcitation process in which a metal electron fills the atom core hole, and the excited atom electron is emitted into the continuum (see Fig. 1). This process is the *exchange* process of the *direct* Auger deexcitation process where interference between both processes has been neglected. The upgrade of the theory would be to include the effect of the ion in the surface barrier and to calculate the surface response function in this way, thus taking into account the presence of the ion in the excitation of the emitted electron.

We have also discussed above that the *direct* Auger deexcitation rate should be larger than the *indirect* one at large atom-surface distances because the *direct* process is basically a *dipolar* excitation of the surface, while the *indirect* is the emission of one atom electron via the tunneling of one metal electron. The dipolar interaction is longer ranged than the electron tunneling, and thus the *direct* term should be larger when the ion is located far from the surface. However, as the atom approaches we have seen that the tunneling process wins over the dipolar excitation: we see this because the *direct* Auger deexcitation rate becomes smaller than the Auger neutralization rate near the surface. Hence, *indirect* Auger deexcitation processes may be very important in particle-surface processes. Work in this direction is in progress.[68]

ACKNOWLEDGMENTS

We thank P. Apell, A. G. Borisov, F. Flores, T. Hecht, R. Monreal, and H. Winter for fruitful discussions. We also thank I.D.R.I.S. for run time in one of its Cray-90 computers. N.L. gratefully acknowledges financial support from the Fundación Ramón Areces. M.A.C. is also grateful for the financial support of the *Unibertsitate and Ikerketa Saila* of the Basque Government. Partial financial support for this work has been obtained from Iberdrola S.A. and the European Union under Contract No. ER-BCHRXCT940571.

[1] H. D. Hagstrum, Phys. Rev. **96**, 325 (1954); **96**, 336 (1954); *Inelastic Ion-Surface Collisions*, edited by N. H. Tolk, J. C. Tully, W. Heiland, and C. W. White (Academic Press, New York, 1977); H. D. Hagstrum, P. Petrie, and E. E. Chaban, Phys. Rev. B **38**, 10 264 (1988).

[2] M. F. A. Harrison, Phys. Rep., Phys. Lett. **37C**, 59 (1978).

[3] P. M. Echenique, F. Flores, and R. H. Ritchie, Solid State Phys. **43**, 229 (1990).

[4] A. G. Borisov, D. Teillet-Billy, and J. P. Gauyacq, Phys. Rev. Lett. **68**, 2842 (1992); A. G. Borisov, D. Teillet-Billy, J. P. Gauyacq, H. Winter, and G. Dierker, Phys. Rev. B **54**, 17 166 (1996).

[5] T. Hecht, A. G. Borisov, and H. Winter, Surf. Sci. **406**, L614 (1998).

[6] N. Lorente, R. Monreal, and M. Alducin, Phys. Rev. A **49**, 4716 (1994).

[7] N. Lorente, M. A. Cazalilla, J. P. Gauyacq, D. Teillet-Billy, and P. M. Echenique, Surf. Sci. Lett. **411** L888 (1998).

[8] H. S. W. Massey, Proc. Cambridge Philos. Soc. **26**, 386 (1930); **27**, 469 (1931).
[9] S. S. Shekhter, J. Exp. Theor. Phys. **7**, 750 (1937).
[10] P. Varga, W. Hofer, and H. Winter, Surf. Sci. **117**, 142 (1982).
[11] P. A. Zeijlmans van Emmichoven, P. A. A. F. Wouters, and A. Niehaus, Surf. Sci. **195**, 115 (1988).
[12] F. W. Meyer, S. H. Overbury, C. C. Havener, P. A. Zeijlmans van Emmichoven, J. Burgdörfer, and D. M. Zehner, Phys. Rev. A **44**, 7214 (1991).
[13] R. Baragiola, in *Low Energy Ion-Surface Interactions*, edited by J. W. Rabalais (Wiley, New York, 1993).
[14] H. Brenten, H. Müller, and V. Kempter, Phys. Rev. Lett. **70**, 25 (1993).
[15] H. H. Brongersma and T. M. Buck, Surf. Sci. **53**, 649 (1975).
[16] W. Heiland and E. Taglauer, Nucl. Instrum. Methods Phys. Res. B **132**, 535 (1976).
[17] R. S. Bhattacharya, W. Eckstein, and H. Verbeek, Surf. Sci. **93**, 563 (1998).
[18] H. Akazawa and Y. Murata, Phys. Rev. B **39**, 3449 (1989).
[19] R. Souda, T. Aizawa, W. Hayami, S. Otani, and Y. Ishizawa, Phys. Rev. B **42**, 7761 (1990); R. Souda, W. Hayami, T. Aizawa, S. Otani, and Y. Ishizawa, *ibid.* **46**, 7315 (1992).
[20] H. Winter, J. Phys.: Condens. Matter **8**, 10 149 (1996).
[21] F. M. Propst, Phys. Rev. **129**, 7 (1963).
[22] J. A. Appelbaum and D. R. Hamann, Phys. Rev. B **12**, 5590 (1975).
[23] E. Hood, F. Boszo, and H. Metiu, Surf. Sci. **161**, 491 (1985).
[24] A. Modinos and S. I. Easa, Surf. Sci. **185**, 569 (1987).
[25] L. A. Salmi, Phys. Rev. B **46**, 4180 (1992).
[26] R. Monreal, Surf. Sci. **388**, 231 (1997).
[27] S. Horiguchi, K. Koyama, and Y. H. Ohtsuki, Phys. Status Solidi B **87**, 757 (1978).
[28] R. Hentschke, K. J. Snowdon, P. Hertel, and W. Heiland, Surf. Sci. **173**, 565 (1986); K. J. Snowdon, R. Hentschke, A. Närmann, and W. Heiland, *ibid.* **173**, 581 (1986).
[29] R. S. Janev and N. N. Nedeljković, J. Phys. B **18**, 915 (1985).
[30] A. A. Almulhem and M. D. Girardeau, Surf. Sci. **210**, 138 (1989).
[31] R. Zimny, Z. L. Mišković, N. N. Nedeljković, and Lj. D. Nedeljković, Surf. Sci. **255**, 135 (1991).
[32] J. M. Schins, R. B. Vrijen, W. J. van der Zande, and J. Los, Surf. Sci. **280**, 145 (1993).
[33] T. Fondén and A. Zwartkruis, Surf. Sci. **269/270**, 601 (1992); A. Zwartkruis and T. Fondén, *ibid.* **290**, 134 (1993); T. Fondén and A. Zwartkruis, Phys. Rev. B **48**, 15 603 (1993); T. Fondén, Ph.D. thesis, Chalmers University, Göteborg, 1993.
[34] F. A. Gutierrez, Surf. Sci. **370**, 77 (1997).
[35] N. Lorente and R. Monreal, Surf. Sci. **370**, 324 (1997).
[36] V. Heine, Phys. Rev. **151**, 561 (1966).
[37] H. Kaji, K. Makoshi, and A. Yoshimori, Surf. Sci. **227**, 138 (1990).
[38] Z. L. Mišković and R. K. Janev, Surf. Sci. **221**, 317 (1989).
[39] H. Kaji, K. Makoshi, and A. Yoshimori, Surf. Sci. **279**, 165 (1992).
[40] U. Wille, Nucl. Instrum. Methods Phys. Res. B **98**, 410 (1995).
[41] F. Guinea, F. Flores, and P. M. Echenique, Phys. Rev. Lett. **47**, 604 (1981).
[42] R. Monreal and N. Lorente, Phys. Rev. B **52**, 4760 (1995).
[43] A. A. Abrikosov, L. P. Gorkov, and I. E. Dzyaloshinski, *Methods of Quantum Field Theory in Statistical Physics* (Dover, New York, 1975).
[44] D. Pines, *Elementary Excitations in Solids* (Addison-Wesley, Reading, MA, 1965).
[45] R. H. Ritchie, Phys. Rev. **106**, 874 (1957); Surf. Sci. Lett. **34**, 1 (1973).
[46] P. J. Jennings, R. O. Jones, and H. Weinert, Phys. Rev. B **37**, 6113 (1988).
[47] M. Aymar and M. J. Crance, J. Phys. B **13**, 2527 (1980).
[48] D. Teillet-Billy and J. P. Gauyacq, Surf. Sci. **239**, 343 (1990).
[49] B. H. Bransden and C. J. Joachain, *Physics of Atoms and Molecules* (Longmans, New York, 1980).
[50] W. Kohn and L. J. Sham, Phys. Rev. A **140**, A1133 (1965).
[51] E. K. U. Gross, J. F. Dobson, and M. Petersilka, in *Density Functional Theory II*, edited by R. F. Nalewajski, Topics in Current Chemistry Vol. 181 (Springer, New York, 1996), p. 81.
[52] M. Petersilka, U. J. Gossmann, and E. K. U. Gross, Phys. Rev. Lett. **76**, 1212 (1996).
[53] A. G. Eguiluz, D. A. Campbell, A. A. Maradudin, and R. F. Wallis, Phys. Rev. B **30**, 5449 (1984).
[54] A. G. Eguiluz, Phys. Rev. B **31**, 3303 (1985).
[55] M. A. Cazalilla, J. Sanchez Dolado, and P. M. Echenique (unpublished).
[56] G. E. Makhmetov, A. G. Borisov, D. Teillet-Billy, and J. P. Gauyacq, Europhys. Lett. **27**, 247 (1994); Nucl. Instrum. Methods Phys. Res. B **100**, 342 (1995).
[57] U. Fano, Phys. Rev. **124**, 1866 (1961).
[58] A. Z. Devdariani, V. N. Ostrovskii, and Yu. N. Sebyakin, Sov. Phys. JETP **44**, 477 (1976).
[59] G. D. Mahan and K. R. Subbaswamy, *Local Density Theory of Polarizability* (Plenum Press, New York, 1990).
[60] K. D. Tsuei, E. W. Plummer, A. Liebsch, K. Kempa, and P. Bakshi, Phys. Rev. Lett. **64**, 44 (1990); K. D. Tsuei, E. W. Plummer, A. Liebsch, E. Pehlke, K. Kempa, and P. Bakshi, Surf. Sci. **247**, 302 (1991).
[61] M. Alducin, Phys. Rev. A **53**, 4222 (1996).
[62] P. M. Echenique, R. M. Nieminen, and R. H. Ritchie, Solid State Commun. **37**, 779 (1981).
[63] C. O. Almbladh and U. von Barth, Phys. Rev. B **13**, 3307 (1976).
[64] R. Diez Muiño, A. Salin, N. Stolterfoht, A. Arnau, and P. M. Echenique, Phys. Rev. A **57**, 1126 (1998).
[65] S. Ossicini and C. M. Bertoni, Europhys. Lett. **1**, 661 (1986).
[66] P. A. Serena, J. M. Soler, and N. García, Phys. Rev. B **37**, 8701 (1988).
[67] I. D. White, R. W. Godby, M. M. Rieger, and R. J. Needs, Phys. Rev. Lett. **80**, 4265 (1998).
[68] N. Lorente, D. Teillet-Billy, and J.-P. Gauyacq (unpublished).